Nuclear Inst. and Methods in Physics Research, A 888 (2018) 147–152

Contents lists available at ScienceDirect

Nuclear Inst. and Methods in Physics Research, A

journal homepage: www.elsevier.com/locate/nima

Operation regimes of a dielectric laser accelerator

Adi Hanuka *, Levi Schächter

Department of Electrical Engineering, Technion, Haifa 32000, Israel

ARTICLE INFO

Keywords:
Dielectric laser accelerator
Efficiency

ABSTRACT

We investigate three operation regimes in dielectric laser driven accelerators: maximum efficiency, maximum charge, and maximum loaded gradient. We demonstrate, using a self-consistent approach, that loaded gradients of the order of 1 to 6 [GV/m], efficiencies of 20% to 80%, and electrons flux of 10^{14} [el/s] are feasible, without significant concerns regarding damage threshold fluence. The latter imposes that the total charge per squared wavelength is constant (a total of 10^6 per μm^2). We conceive this configuration as a zero-order design that should be considered for the road map of future accelerators.

The road map for a future linear collider was drawn recently [1] and it includes several schemes: plasma wake field acceleration (PWFA) [2], laser wake-field acceleration (LWFA) [3,4] and two-beam accelerator (TBA) [5,6]. In the first case a short electron bunch generates a *plasma* wake and the latter accelerates a trailing bunch. A similar wake is generated by a laser pulse in the second paradigm. In the framework of the third one, a driving bunch generates an *electromagnetic* wake which in turn accelerates a trailing bunch. Concerns of space-charge effects, low efficiency and modest luminosity, excluded the dielectric laser accelerator (DLA) from the list of viable alternatives. While the gradients experimentally demonstrated by the plasma based paradigms, are incredibly high comparing to what was conceived feasible before the pioneering work of Tajima and Dawson [7], there is still a long and rough road to overcome plasma instabilities at the necessary repetition rate and positron acceleration in the framework of these schemes.

Recent developments in fabrication [8,9] and experimental demonstrations [10,11] showed a realization towards high gradients of DLA (~1 GV/m), dictated by the damage fluence threshold that materials can withstand. However, in order for the DLA to be further considered as a viable alternative, even higher gradients are required, as well as a considerable amount of accelerated charge with decent efficiency. Therefore, understanding its optimal operation regimes opens up a pathway to further DLA applications. This optimal operation is facilitated by the fact that the dielectric structure is not exposed to the entire laser energy flux since a significant part of the latter is absorbed by the electrons – thus the required high efficiency.

In this study we present the results of a self-consistent optimization of the operating parameters of an idealized acceleration module [12]. Subject to some simplifying assumptions that will be specified subsequently, our analysis indicates that loaded gradients approaching the 6 GV/m level are definitely feasible, efficiencies exceeding 50% are achievable and with current laser technology the required luminosity of a linear collider is already in reach. It is important to emphasize already at this stage that high efficiency implies significantly lower electromagnetic energy density in the dielectric near the vacuum tunnel thus reducing the concerns of fluence damage or other non-linear effects.

Our analysis assumes a 1 μm laser though indications (shown subsequently) are that a CO_2 laser (10.6 μm) may perform reasonably well. For the numerical examples presented, the acceleration structure is adopted to be a dielectric $(\varepsilon_r = 2.1)$ loaded waveguide, whereby for a given dielectric (fused Silica) and vacuum tunnel radius (R_{int}), the external radius (R_{ext}) is set by imposing single mode (TM_{01}) operation and phase velocity equal to the speed of light in vacuum. Note that in our specific configuration, imposing the group velocity sets R_{int} and vice versa. This choice of structure was made because of the analytic relations between the various parameters. Further, the laser pulse is conceived to be ideal in the sense that its rise and fall times are negligible comparing to its duration (τ_p).

With regards to the electron bunch, it is conceived to consist of a *single* point-charge (q) ignoring in the process space-charge effect. We discuss the latter in the last section and we present some of the main results of our analysis in the case of a train of micro-bunches; in any event, the single macro-particle case represents the best case scenario. We consider only the case of full overlap between the laser pulse that propagates at group velocity $c\beta_{\mathrm{gr}} < c$ and the relativistic bunch that moves practically at the speed of light (c). Furthermore, both the laser

* Corresponding author.
E-mail address: adiha@tx.technion.ac.il (A. Hanuka).

https://doi.org/10.1016/j.nima.2018.01.060
Received 27 November 2017; Accepted 17 January 2018
Available online 2 February 2018
0168-9002/

pulse and the wake leave the accelerating module before the next laser pulse fills in.

Lastly, additional assumptions of the present study: (i) for the structure of interest, the wake parameter (κ) is known, and it determines the intensity of the decelerating wakefield in terms of the driving charge. The wake's projection on the first accelerating mode is $\kappa_1 = W_1\kappa < \kappa$. (ii) The coupling of power into the accelerating module is 100% efficient. (iii) At the laser's wavelength ($\lambda = 1$ μm), the dependence of the Damage Threshold Fluence $F(\tau_p)$ on the pulse duration (τ_p) in Fused Silica, is known [13]:

$$F\left(\tau_p\right) = \left[\frac{\mathrm{J}}{\mathrm{cm}^2}\right]\begin{cases} 1.44\tau_p^{1/2} & \tau_p\,[\mathrm{ps}] > 10 \\ 2.51\tau_p^{1/4} & 0.4 < \tau_p\,[\mathrm{ps}] < 10 \\ 2 & \tau_p\,[\mathrm{ps}] < 0.4 \end{cases} \tag{1}$$

Two observations warrant attention here: at very short pulse duration ($\tau_p < 0.4$ [ps]) the Damage Threshold Fluence (DTF) is limited to 2 J/cm^2 whereas for long pulse duration ($\tau_p > 10$ [ps]) the DTF exceeds 5 J/cm^2.

Based on the assumptions above, we may formulate the constraints that limit the number of degrees of freedom in our model. While the full analysis is presented in our previous work [12], in what follows we briefly summarize the main steps. We start with the observation that virtually in all dielectric based acceleration structures the energy flux reaches its maximum at the vacuum-dielectric interface. If we ignore the effect of the wake on the accelerating mode, the maximum energy flux $\left(S_z^{\max}\right)$ in the dielectric is proportional to the square accelerating gradient on axis $\left(G_0\right)$. Note that for a given gradient, the larger the dielectric coefficient, the lower the energy flux.

In the framework of this study we consider a reduction in the maximum energy flux due to the *wakefield* on the fundamental mode (denoted as κ_1). Thus we replace $G_0 \to G_0 - \kappa_1 q$; this peak value of the energy flux is limited by the Damage Threshold Fluence (DTF) that the material can withstand, thus

$$\frac{F\left(\tau_p\right)}{\tau_p} \equiv S_z^{\max} = \frac{1}{2\eta_0\varepsilon_r}\left(\frac{\pi R_{\mathrm{int}}}{\lambda}\right)^2\left(G_0 - \kappa_1 q\right)^2. \tag{2}$$

Clearly, for establishing the DTF we need to know the pulse duration. The latter, in turn, is determined, based on the overlap condition specified above, in terms of the group velocity and the geometric interaction length (L_{geo})

$$\tau_p = \frac{L_{\mathrm{geo}}}{c}\left(\beta_{\mathrm{gr}}^{-1} - 1\right). \tag{3}$$

This last parameter determines also the energy gained, $mc^2\Delta\gamma$, along the module in terms of the *loaded gradient* on the bunch $G_0 - \kappa q$,

$$mc^2\Delta\gamma = e\left(G_0 - \kappa q\right)L_{\mathrm{geo}}. \tag{4}$$

In this set of non-linear equations, for any given set of parameters $\left(\Delta\gamma,\ R_{\mathrm{int}}\right)$, there are two unknowns: the unloaded gradient G_0 and the bunch charge q. Explicitly, for a pre-selected charge q the unloaded gradient is a solution of Eq. (2) with $\tau_p = mc^2\Delta\gamma\left(\beta_{\mathrm{gr}}^{-1} - 1\right)/ec\left(G_0 - \kappa q\right)$ and vice-versa, for a prescribed unloaded gradient, the charge is a solution of Eq. (2).

With these two quantities established $\left(G_0, q\right)$, the efficiency may be readily calculated [14]

$$\eta_1 = \frac{q\left(G_0 - \kappa q\right)L_{\mathrm{geo}}}{U_{\mathrm{EM}}} = 4\eta_{\max}\frac{\kappa q}{G_0}\left(1 - \frac{\kappa q}{G_0}\right) \tag{5}$$

where U_{EM} is the electromagnetic energy, and the maximum efficiency is $\eta_{\max} \equiv \kappa_1/\kappa$. This maximum efficiency imposes an additional constraint on the choice of G_0 or q. For example, the requirement of operating at maximum efficiency, determines both the charge and the gradient. Other constrains may lead to different regimes of operation – as discussed subsequently.

Before we proceed to analysis of the various feasible regimes of operation, it warrants to emphasize that maximum efficiency is smaller than 10% in the case of Bragg reflections waveguide, either planar (PBA) or cylinder (CBA) for typical existing materials (Silica and Zirconia) – see Fig. 1 (red and green curves). Similar maximum efficiency (6%) was estimated [15] for honey-comb structure (black star), whereas in the present case (dielectric loaded waveguide – blue and purple curves) the maximum efficiency reaches 62% for the same group velocity $\beta_{\mathrm{gr}} = 0.6$ as in [15] for $R_{\mathrm{int}}/\lambda = 0.44$, $\lambda = 1$ μm. Moreover, preliminary estimates [16] indicate that meta materials with characteristics similar to "ferromagnetic" properties may exceed this value and reach efficiencies in excess of 90% for loaded waveguide, or 30% for Bragg structures. This is a major improvement over the present situation that beyond maximum efficiency improvement, leads to almost one order of magnitude in the gradient, as will be demonstrated next.

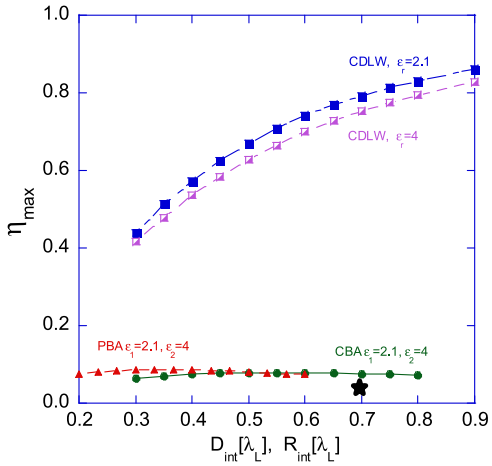

Fig. 1. (Color online) Maximum efficiency as a function of the vacuum clearance for three types of structures; (i) Cylinder Dielectric Loaded Waveguide (CDLW) with either Silica (blue) or Zirconia (purple) loading, (ii) Planar or (iii) Cylinder Bragg Accelerator (PBA or CBA) with alternating layers of Silica and Zirconia. The latter two structures present the lowest efficiency (~10%). The black star represents the honey-comb [17] fiber.

Table 1
Parameters of the Laser and the envisaged structure.

Parameter	Symbol	Value
Laser		
Laser wavelength [μm]	λ	1
Group velocity	β_{gr}	0.74
Phase velocity	β_{ph}	1.0
Interaction impedance [Ω]	Z_{int}	173
Laser power [kW]	P_{L}	$7.2\left\{\mathrm{G}_0\left[\frac{\mathrm{GV}}{\mathrm{m}}\right]\right\}^2$
Structure		
Internal radius [λ]	R_{int}	0.7
External radius [λ]	R_{ext}	0.82
Dielectric constant	ε_r	2.1
Wake coefficient $\left[\frac{\mathrm{GV}}{\mathrm{m\cdot pC}}\right]$	κ	36
Energy gain required	$\Delta\gamma$	1.7
Maximum efficiency [%]	$\eta_{\max}$	80

In order to determine an *optimal* operation regime, we consider the effect of the accelerating module's length on the gradient and efficiency given the intrinsic set of parameters in Table 1. The results of such self-consistent analysis are presented in Fig. 2: unloaded gradient G_0 (top) and loaded gradient G_{Loaded} (bottom) versus the efficiency η normalized to its maximum value (80%) for various values of geometrical length (colorbar). Notably, both the efficiency and unloaded gradient reach maximum. However, maximum efficiency, maximum unloaded (corresponds to maximum charge) and loaded gradients occur for different geometrical lengths, and therefore cannot be satisfied together. In what follows, we examine the *three* different regimes – maximal efficiency, maximal charge, and maximal loaded gradient.

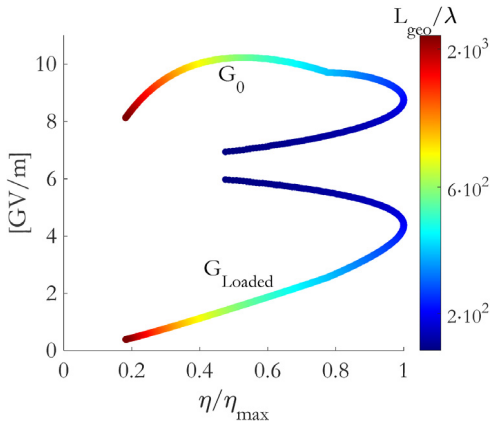

Fig. 2. (Color online) Unloaded (top) and loaded (bottom) gradients versus the efficiency normalized to its maximum value (80%) for various values of geometrical length (colorbar). Notably, both the efficiency and unloaded gradient reach maximum. However, maximum efficiency, maximum unloaded gradient (corresponds to maximum charge), and maximum loaded gradient occur for different geometrical lengths, and therefore cannot be satisfied together.

Fig. 2 clearly reveals that for a geometric length of about 200 wavelengths (0.2 [mm]), the *maximal efficiency* reaches the value (80%) and the *unloaded* gradient is 8.7 [GV/m] whereas the *loaded* value is 4.3 [GV/m]. The difference between the two is because of the relatively high charge in the bunch $q \sim 0.12$ [pC] $\sim 0.75 \times 10^6 e$, the corresponding power is 0.56 [MW] for a time duration of $\tau_p \sim 0.24$ [ps]- thus the electromagnetic energy in a single pulse 0.13 [μJ]. In order to satisfy the luminosity requirements of the international linear collider (ILC) [18], the electrons' flux needs to be $\sim 10^{14}$ el/s. Therefore, we need a *repetition rate* of approximately 100 MHz, implying an average power of 13 W. Assuming a spacing between two modules of the same order of magnitude as the length of a single module, then in one meter of the collider there are 2500 modules and consequently, the average power required in *one meter* is about 33 [kW]. This value is compatible with today's power obtained from several fiber lasers in both continuous-wave (cw) and high repetition rate of pulsed operation [19,20].

In the previous paragraph we were biased by maximum efficiency. Now we repeat the evaluation focusing on *maximum charge* (or equivalently unloaded gradient). For the same parameters in Table 1, for a geometric length of about 750 wavelengths (0.75 [mm]) - see Fig. 2 - the *unloaded* gradient reaches its maximum (10 [GV/m]) whereas the *loaded* gradient is 1.2 [GV/m], and the *efficiency* value is 32%. The difference between the two gradients is because of the relatively high charge in the bunch $q \sim 0.24$ [pC] $\sim 1.5 \times 10^6 e$, the corresponding power is 0.73 [MW] for a time duration of $\tau_p \sim 0.88$ [ps]- thus the electromagnetic energy in a single pulse 0.65 [μJ]. Assuming a repetition rate of 100 MHz (to satisfy the electrons' flux of $\sim 10^{14}$ el/s), the average power is 65 [W] – for one module. Assuming a spacing between two modules of the same order of magnitude, then in one meter of the collider there are 667 modules and consequently, the average power required in *one meter* is about 43 [kW].

A third set of parameters leads to *maximum loaded gradient*. For the same parameters in Table 1, for a geometric length of 0.14 [mm] (see Fig. 2) unloaded gradient reaches 6.6 [GV/m] whereas the *loaded* gradient is 6.2 [GV/m], and the efficiency is ~20%. The relatively small difference between the two gradients is due to the low bunch charge $q \sim 0.012$ [pC] $\sim 0.07 \times 10^6 e$, the corresponding power is 0.32 [MW] for a time duration of $\tau_p \sim 0.16$ [ps]- thus the electromagnetic energy in a single pulse 0.05 [μJ]. As previously, assuming a repetition rate of 100 MHz, the average power is 5 [W] – for one module. Assuming a spacing between two modules of the same order of magnitude as the length of the module, then in one meter of the collider there are 3570 modules and consequently, the average power required in *one meter* is about 18 [kW]. Due to the low charge, higher repetition rate is required in order to satisfy the electrons' flux of $\sim 10^{14}$ el/s. All three regimes are summarized in Table 2 for two cases: (i) same repetition rate of 100 MHz, and (ii) same electron flux of $1 \cdot 10^{14}$ el/s.

Strictly speaking, from the perspective of the zero-order parameters, gradient, efficiency, luminosity and damage threshold fluence, the present self-consistent analysis clearly indicates that neither of the four parameters pose an inherent impediment. In fact, this analysis reveals that, with proper choice of parameters, loaded gradient in excess of 4 [GV/m] is feasible, with a theoretical efficiency of about 80% and the averaged power required to satisfy the luminosity constraints translated to in 1m long segment are within reach.

The set of parameters that facilitate maximum loaded gradient makes the constraint (repetition rate) necessary to satisfy the electrons' flux imposed by the luminosity very stringent. A different choice of intrinsic parameters $(\Delta\gamma, R_{\text{int}})$ may release somewhat the constraint – as indicated in Table 3. We examined various combinations of energy gain $(\Delta\gamma = 1.7, 6)$, and two different internal radii $(R_{\text{int}} = 0.8\lambda, 0.7\lambda)$. A structure with internal radius $R_{\text{int}} = 0.8\lambda$ has maximum efficiency of 83% and group velocity of 0.78 – nearly the same as compared with $R_{\text{int}} = 0.7\lambda$ (80% and 0.74 respectively). However, as shown subsequently, increasing the vacuum core's radius or reducing the energy gain have the potential to readily retain an electron flux of $\sim 10^{14}$ at 100 MHz. Each parameters' choice corresponds to a different fluence regime as might be inferred from Eq. (1).

Three facts are evident: first, for the parameters in Table 1, compromising the maximum loaded gradient (3.5 [GV/m] as compared with ~6.2 [GV/m]) could facilitate the electron flux of 10^{14} at 100 MHz. Second, wider vacuum tunnel could potentially readily satisfy both high loaded gradient and the required electron flux. For example, for $R_{\text{int}} = 0.8\lambda$ it is feasible to satisfy the latter, together with higher loaded gradient (4.4 [GV/m] as compared with 3.5 [GV/m]). This result is more pronounced for higher dielectric coefficients (not shown here). Third, as the required energy gain is higher, it is impossible to reach high loaded gradient and to satisfy the required electron flux at the same time. Moreover, for higher energy gain, the structure's length and the pulse duration should be one–two orders of magnitude longer.

In addition to increasing the vacuum tunnel, longer wavelengths will also increase the amount of charge in the bunch. Assuming the same *fluence* dependence as in Eq. (1), Fig. 3a shows the number of electrons N_{el} in a bunch for three wavelengths as a function of loaded gradient for $R_{\text{int}} = 0.5\lambda$. Clearly, wavelengths of 10 μm (dotted blue) or 2 μm (solid red) facilitate order of magnitude higher charge than wavelength of 1 μm (dashed green). Since the number of electrons in a single bunch is higher in longer wavelengths, satisfying electron flux of 10^{14} electrons per second, requires lower repetition rate, and thus the average power would be lower as well.

As could be inferred from Fig. 3a, the number of electrons is scaled like the square of the wavelength, namely the quantity $\overline{N}_{\text{el}} \equiv N_{\text{el}}/\lambda^2\ [\mu\text{m}^2]$ is constant, assuming the same fluence dependence for all wavelengths. We are not aware of experimental data similar to that in Ref. [13] for CO_2 laser (10 μm). However, in order to get a flavor as of the general trend, we assume that the fluence damage for short pulses is 0.3 J/cm^2 or 0.8 J/cm^2 instead of 2 J/cm^2, and it has the same dependence on the pulse duration. The self-consistent analysis with the scaled fluence (solid turquoise or dashed purple respectively) results not only in a reduced number of electrons, but also the loaded gradient attainable is much smaller.

Regardless of the wavelength (1 μm or 10 μm), an order of 10^5–10^6 electrons in a bunch give rise to *space-charge* force that might be a serious impediment. Therefore, there exists a serious need for a focusing system. Imposing that the confining force of a focusing lattice is stronger than repelling force of the charged particles, it sets a limit on the total number of electrons in a bunch. The latter is determined by the momentum of the electrons and the energy density of the focusing system. For example,

Table 2
A comparison between the different regimes: maximum unloaded/loaded gradient and maximal efficiency regime.

Parameter	Max. efficiency	Max. charge	Max. loaded gradient
Efficiency [%]	80%	32%	20%
Unloaded gradient [GV/m]	8.7	10	6.6
Loaded gradient [GV/m]	4.3	1.2	6.2
Charge [pC]	0.12	0.24	0.012
# of electrons 10^6	0.75	1.5	0. 07
Single Pulse Power [MW]	0.56	0.73	0.32
Structure length [mm]	0.2	0.75	0.14
Pulse duration [ps]	0.24	0.88	0.16
EM energy [μJ/pulse]	0.13	0.65	0.05
# of modules per meter	2500	667	3570
Case 1 (rep. rate):			
Rep. Rate [MHz]	100	100	100
Average power [W]	13	65	5
Average power per meter [kW/m]	33	43	118
Electrons flux [el/sec] 10^{14}	0.75	1.5	0.07[a]
Case 2 (e- flux):			
Rep. Rate [MHz]	140	70	1400[b]
Average power [W]	18	45	74
Average power per meter [kW/m]	46	30	264
Electrons flux [el/sec] 10^{14}	1	1	1

[a] At maximum loaded gradient the electrons' flux imposed by the ILC luminosity is one order of magnitude lower. In the other two cases there seems to be excellent match between the needs and what proves theoretically to be achievable.

[b] Compatible laser is not within reach, however new technologies will emerge and hopefully they will approach the required values.

Table 3
Regime parameters for various combinations of energy gain ($\Delta\gamma$) and internal radius (R_{int}) for a laser with repetition rate of 100 MHz.

Internal radius [λ]	0.8		0.7	
Energy gain	1.7	6	1.7	6
Pulse duration [ps]	0.18	3.7	0.23	6.5
Fluence [J/cm^2]	2	3.5	2	4
Structure length [mm]	0.2	4	0.25	5.5
Efficiency [%]	83%	40%	74%	33%
Unloaded gradient [GV/m]	9	5.3	9.4	4.7
Loaded gradient [GV/m]	4.4	0.76	3.5	0.5
# of electrons [10^6]	1	1	1	0.7

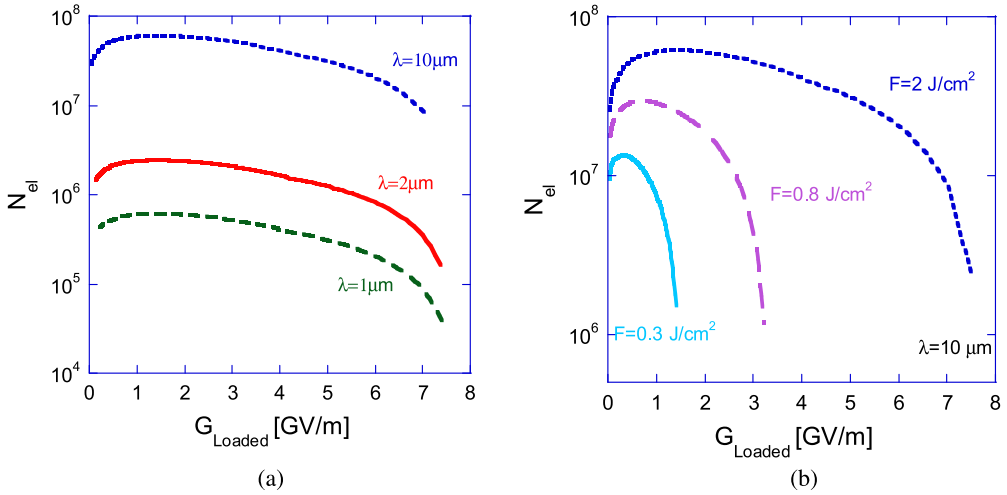

Fig. 3. (Color online) (3a) Total number of electrons in a train of microbunches as a function of the loaded gradient for three wavelengths: 10 μm (dotted blue), 2 μm (solid red) and 1 μm (dashed green) – assuming the same fluence dependence. (3b) Total number of electrons for $\lambda = 10$ μm as a function of loaded gradient for three damage fluence scaling: Eq. (1) (dotted blue), the latter scaled by a 0.15 factor (solid turquoise) or by a 0.4 factor (dashed purple).

assuming the SLAC NLCTA beam (60 MeV) and a typical solenoidal magnetic field of $B = 0.5$ T, the electron density is

$$n_{\text{el}} \leq \frac{2\varepsilon_0 m\gamma^3}{e^2}\left(\frac{1}{2}\frac{eB}{m\gamma}\right)^2 \simeq 10^{14}\ \text{cm}^{-3}. \tag{6}$$

For a typical bunch radius of $r_b = 0.2\lambda$, and bunch longitudinal length $\sigma_z = 0.1\lambda$, the total number of electrons in a bunch is nearly one!

Fig. 4 shows the maximum charge that could be transported in a focusing lattice as a function of the beam kinetic energy $E_k = (\gamma - 1)\,mc^2$ for four types of focusing lattices: Einzel lens (green), Solenoid (red), Electric or Magnetic quadrupole (blue or turquoise respectively). The number of electrons is given by

$$N_{\text{el}} = \frac{1}{2}\gamma^3\beta^2 Q_{\max}\frac{\sigma_z}{r_{\text{el}}} \tag{7}$$

Table 4
Maximum perveance for each focusing system as well as typical values for the parameters used for Fig. 4. Beam radius $r_b = 0.2$ μm, Pipe radius $r_p = 2$ μm.

Focusing system	Maximum perveance $Q_{\max}$	Parameter	Symbol	Value
Einzel lens	$\frac{3\pi^2}{2}\left(\frac{qV}{mc^2\beta^2}\right)^2\left(\frac{r_b}{L}\right)^2$	Voltage relative to ground Length	V $2L$	15 keV 1mm
Solenoid	$\left(\frac{eBr_b}{2\gamma\beta mc}\right)^2$	Magnetic field	B	0.5 T
Electric Quadrupole	$\frac{\eta\sigma_0}{\sqrt{2}\pi}\mathrm{sinc}\left(\eta\frac{\pi}{2}\right)\frac{e2V}{\gamma\beta^2mc^2}\left(\frac{r_b}{r_p}\right)^2$	Occupancy Maximum phase advance [22] Voltage relative to ground	η σ_0 V	0.5 85° 15 keV
Magnetic Quadrupole	$\frac{\eta\sigma_0}{\sqrt{2}\pi}\mathrm{sinc}\left(\eta\frac{\pi}{2}\right)\frac{Br_p}{[B\rho]}\left(\frac{r_b}{r_p}\right)^2$	Occupancy Maximum phase advance [22] Magnetic field Beam rigidity	η σ_0 B $[B\rho]$	0.5 85° 0.1 T $\gamma m\beta c/e$

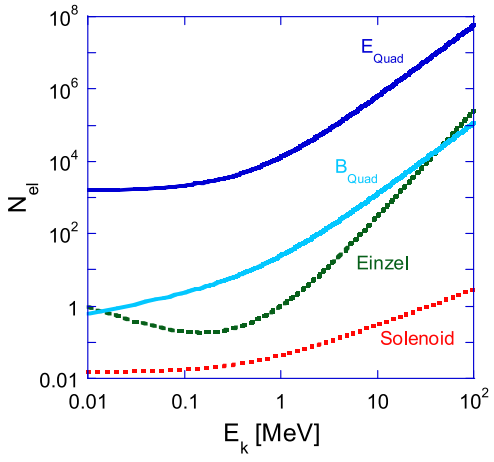

Fig. 4. (Color online) Maximum number of electrons in a bunch as a function of its kinetic energy for four lattices: Einzel lens (green), Solenoid (red), Electric or Magnetic quadrupole (blue or turquoise respectively).

where $Q_{\max}$ is the maximum perveance for each focusing system, β is the electron normalized velocity and r_{el} is the classical radius of the electron. Table 4 summarizes analytical formula of the maximum perveance for each focusing system as well as typical values for the parameters used for Fig. 4.

It is evident that Electric Quadrupole would facilitate the highest amount of charge. The applied voltage will be limited by the distance between two adjacent electrodes, such that breakdown is avoided. Therefore, it seems inevitable to split the bunch into a train of bunches in order to weaken the space-charge and to somewhat increase the total amount of accelerated charge. In our previous work [21] for optimal accelerator design for a train of M microbunches, the average charge density per microbunch decreases like M, while the total amount of charge in the train virtually, does not change. This space-charge reduction comes at the expense of the maximum efficiency, which is at least 20% lower than the single bunch configuration.

In conclusion, we showed the properties of three operation regimes in dielectric laser driven accelerators: maximum efficiency, maximum charge, and maximum loaded gradient. For each regime, our self-consistent analysis considered the reduction of the beam loading on the material. We showed the trade-offs between the regimes, wherein loaded gradients of the order of 1.2 to 6.2 [GV/m] and efficiencies of 20 to 80% are feasible. This, without serious concerns regarding damage threshold fluence. With regards to the maximum loaded gradient regime, achieving an electron flux of 10^{14} [el/s] to satisfy the luminosity requirements with a reasonable repetition rate laser is highly stringent. This constraint might be somewhat released by properly selecting intrinsic parameters such as the structure's radius and required energy gain.

We further showed that increasing the amount of charge in the bunch might be readily facilitated by increasing the wavelength. However, the total charge per squared wavelength remains the same – an order of 10^6 electron per wavelength squared (expressed in μm). This amount of charge gives rise to space charge forces that might be a serious impediment. Imposing a confining force of a focusing lattice sets an upper limit on the amount of charge, depending on the focusing system. By investigating four different focusing lattices, we showed that *Electric Quadrupole* would facilitate the highest amount of charge. Nevertheless, it seems inevitable to split the bunch into a train of bunches in order to weaken the space charge effect. We conceive this configuration as a zero-order design for a future Dielectric Laser Accelerator.

References

[1] E. Colby, L. Len, Roadmap to the future, Rev. Accel. Sci. Technol. 9 (2016) 1–18.
[2] M. Litos, E. Adli, W. An, C.I. Clarke, C.E. Clayton, S. Corde, J.P. Delahaye, R.J. England, A.S. Fisher, J. Frederico, S. Gessner, S.Z. Green, M.J. Hogan, C. Joshi, W. Lu, K.A. Marsh, W.B. Mori, P. Muggli, N. Vafaei-Najafabadi, D. Walz, G. White, Z. Wu, V. Yakimenko, G. Yocky, High-efficiency acceleration of an electron beam in a plasma wakefield accelerator, Nature 515 (7525) (2014) 92–95.
[3] C. Joshi, V. Malka, Focus on laser- and beam-driven plasma accelerators, New J. Phys. 12 (2010).
[4] E. Esarey, C.B. Schroeder, W.P. Leemans, Physics of laser-driven plasma-based electron accelerators, Rev. Modern Phys. 81 (3) (2009) 1229–1285.
[5] S.Y. Kazakov, S.V. Kuzikov, Y. Jiang, J.L. Hirshfield, High-gradient two-beam accelerator structure, Phys. Rev. Spec. Top. - Accel. Beams 13 (7) (2010) 1–14.
[6] H. Braun, R. Corsini, J.P. Delahaye, A. De Roeck, S. Doebert, G. Geschonke, A. Grudiev, C. Hauviller, B. Jeanneret, E. Jensen, et al., CLIC 2008 parameters, CLIC-Note 764 (2008) 1–41.
[7] T. Tajima, J.M. Dawson, Laser electron accelerator, Phys. Rev. Lett. 43 (4) (1979) 267–270.
[8] A. Ceballos, R.L. Byer, K.J. Leedle, E. Peralta, O. Solgaard, K. Soong, R.J. England, I. Makasyuk, K.P. Wootton, Z. Wu, M. Park, A. Hanuka, F.U. Erlangen-nuernberg, Fabrication and demonstration of a silicon buried grating accelerator, no. 1.
[9] E.A. Peralta, R. Byer, Fabrication and measurement of dual layer silica grating structures for direct laser acceleration, in: Proc. 2011 Part. Accel. Conf., 2011, pp. 280–282.
[10] K.P. Wootton, Z. Wu, B.M. Cowan, A. Hanuka, I.V. Makasyuk, E.A. Peralta, K. Soong, R.L. Byer, R.J. England, Demonstration of acceleration of relativistic electrons at a dielectric microstructure using femtosecond laser pulses, Opt. Lett. 41 (12) (2016).
[11] E.A. Peralta, K. Soong, R.J. England, E.R. Colby, Z. Wu, B. Montazeri, C. McGuinness, J. McNeur, K.J. Leedle, D. Walz, E.B. Sozer, B. Cowan, B. Schwartz, G. Travish, R.L. Byer, Demonstration of electron acceleration in a laser-driven dielectric microstructure, Nature 503 (7474) (2013) 91–94.
[12] A. Hanuka, L. Schächter, Optimized operation of laser driven accelerator: Single bunch, Phys. Rev. Accel. Beams (2017) Submitted.
[13] B.C. Stuart, M.D. Feit, A.M. Rubenchik, B.W. Shore, M.D. Perry, Laser-induced damage in dielectrics with nanosecond to subpicosecond pulses, Phys. Rev. Lett. 74 (12) (1995) 2248–2251.
[14] K. Bane, G. Stupakov, Impedance of a rectangular beam tube with small corrugations, Phys. Rev. Spec. Top. - Accel. Beams 6 (2) (2003) 24401.
[15] R.H. Siemann, Energy efficiency of laser driven, structure based accelerators, Phys. Rev. Spec. Top. - Accel. Beams 7 (6) (2004) 61303.

[16] A. Hanuka, E. Goldemberg, A. Zilka, L. Schächter, Artificial materials for structure-based laser acceleration, in: Proc. of AAC16, 2017, p. 60008.
[17] X. Lin, Photonic band gap fiber accelerator, Phys. Rev. Spec. Top. - Accel. Beams 4 (5) (2001) 51301.
[18] International Linear Collider Reference Design Report, ILC Global Design Effort and World Wide Study, 2007.
[19] D.J. Richardson, J. Nilsson, W.A. Clarkson, High power fiber lasers: current status and future perspectives, J. Opt. Soc. Amer. B 27 (11) (2010) B63–B92.
[20] P.F. Moulton, G.A. Rines, E.V. Slobodtchikov, K.F. Wall, G. Frith, B. Samson, A.L.G. Carter, Tm-doped fiber lasers: Fundamentals and Tm-doped fiber lasers: Fundamentals and power scaling, IEEE J. Sel. Top. Quantum Electron. 15 (November 2016) (2009) 85–92.
[21] A. Hanuka, L. Schächter, Efficiency and Optimum charge in Bragg accelerator, in: proc. of IPSTA-The 16th Israeli Plasma Science and Applications Conference, 2014, pp. 73–74.
[22] S.M. Lund, S.R. Chawla, Space-charge transport limits of ion beams in periodic quadrupole focusing channels, Nucl. Instrum. Methods Phys. Res. Sect. A 561 (2) (2006) 203–208.